NIH Public Access
Author Manuscript
J Neuroimmune Pharmacol. Author manuscript; available in PMC 2014 December 01.

Published in final edited form as:
J Neuroimmune Pharmacol. 2013 December ; 8(5): 1197–1209. doi:10.1007/s11481-013-9511-3.

Alterations in the levels of vesicular trafficking proteins involved in HIV replication in the brains and CSF of patients with HIV-associated neurocognitive disorders

Jerel Fields[1,*], **Wilmar Dumaop**[1,*], **Anthony Adame**[2], **Ronald J. Ellis**[2], **Scott Letendre**[3], **Igor Grant**[4], and **Eliezer Masliah**[1,2]

[1]Department of Pathology, University of California San Diego, La Jolla, CA 92093, USA

[2]Department Neurosciences, University of California San Diego, La Jolla, CA 92093, USA

[3] Department Medicine, University of California San Diego, La Jolla, CA 92093, USA

[4]Department Psychiatry, University of California San Diego, La Jolla, CA 92093, USA

Abstract

Human immunodeficiency virus (HIV) associated neurocognitive disorders (HAND) remain prevalent despite improved antiretroviral therapies. A HAND-specific biomarker indicative of neuropsychological impairment (NPI) would give insight into disease progression and aid clinicians in designing therapy. Endosomal sorting complex required for transport (ESCRT) proteins such as tumor susceptibility gene (TSG)-101, vacuolar protein sorting (VPS)-4 and LIP-5 are important for HIV replication and recently antiviral interferon stimulated gene (ISG)-15 was proposed as a biomarker for CNS injury. Here, we analyzed a well-characterized cohort of HIV+ cerebral spinal fluid (CSF) and postmortem brain specimens for multiple vesicular trafficking proteins and a related innate immune protein, ISG-15, TSG-101, VPS-4 and LIP-5. All protein levels trended higher with increased NPI and neuropathology. ISG-15 CSF levels were increased in HIV encephalitis (HIVE) compared to normal cases, and three quarters of HIVE samples had above average CSF ISG-15 levels. VPS-4 CSF levels were increased in NPI/NPI-O compared to normal patients. VPS-4 CSF levels in HIV-associated dementia were equivalent to that of normal patients. LIP-5 CSF levels positively correlate with ISG-15 levels, and higher than average ISG-15 levels indicate elevated viral load. Immunoblot and immunohistochemical analyses show increased expression of ISG-15, VPS-4 and LIP-5 in neuronal cell bodies and astroglial cells. ESCRT protein CSF levels analyzed in conjunction with viral load may be indicative of NPI stage, and may aid in the diagnosis and design of therapies for HIV patients. Further studies on the ESCRT protein expression during HIV infection may lead to a promising biomarker for predicting progression of NPI.

Keywords

HIV; biomarker; ESCRT; ISG-15; VPS-4; LIP-5

Corresponding author: Eliezer Masliah, Department of Neurosciences, School of Medicine, University of California San Diego, 9500 Gilman Dr., MTF 348, La Jolla, CA 92093-0624, USA. Office: (858) 534 8992 Fax: (858) 534 6232; emasliah@ucsd.edu.
*Authors contributed equally to manuscript

Conflict of interest

The authors of this manuscript declare that there are no actual or potential conflicts of interest. The authors affirm that there are no financial, personal or other relationships with other people or organizations that have inappropriately influenced or biased their research.

NIH-PA Author Manuscript
NIH-PA Author Manuscript
NIH-PA Author Manuscript

NIH-PA Author Manuscript

NIH-PA Author Manuscript

NIH-PA Author Manuscript

Introduction

HIV infection remains a monumental challenge with over 30 million infected people worldwide (2007). Effective drug regimens are extending patient life into unchartered territories; chronic HIV infection and antiretroviral therapies (ART) have been documented to affect mitochondria function, insulin resistance and lipoatrophy (Montaner et al., 2003; Havlir and Currier, 2006; Sharma et al., 2013). Despite reduced peripheral viral load and lower rates of HIV-associated dementia (HAD), milder forms of HIV associated neurocognitive disorders (HAND) persist (Heaton et al., 2010; Heaton et al., 2011). HAND are initiated when HIV-infected monocytes cross the blood-brain-barrier (BBB), release progeny virus and cytokines/chemokines, and ultimately infecting and activating bystander cells (Budka et al., 1987; Gendelman et al., 1994; Cherner et al., 2007). Currently HAND are occurring at the same or increasing levels in this growing population of aging HIV patients (Heaton et al., 2010; Joska et al., 2010). New diagnostic tools and effective therapies will be crucial to controlling HAND in the aging HIV-infected population.

HAND progression is variable throughout the population of HIV patients and does not always correlate with viral load (Heaton et al., 2008). A biomarker indicative of early stage HAND would allow clinicians and patients to take preventive steps to ease the burden of neurocognitive impairment (Pendyala et al., 2007). Pre-ART markers, such as beta-2-microglobulin, correlated with neurocognitive impairment, but more effective therapies have changed the pathology of chronic infection (Strathdee et al., 1996). Recent studies have shown peripheral markers, such as CD14 (Lichtfuss et al., 2011), CD163 (Merino et al., 2011) and the insulin receptor (Gerena et al., 2012), correlate with neurocognitive impairment, but a marker for early stage HAND that is specific for the CNS remains elusive. More recently, interferon stimulated gene-15 has been implicated as a possible biomarker for HAND (Everall et al., 2005; Gelman et al., 2012; Wang et al., 2012).

HIV highjacks the endosomal-sorting complex required for transport (ESCRT) pathway to facilitate efficient viral replication (Pincetic et al., 2010; Kuang et al., 2011). Interferon-stimulated gene (ISG)-15 prevents ESCRT protein tumor susceptibility gene (TSG)-101 from associating with HIV gag and subsequent viral budding (Okumura et al., 2006; Pincetic et al., 2010; Kuang et al., 2011; Grover et al., 2013; Poteet et al., 2013). *In vitro*, upregulating ISG-15, via interferon (ifn) or overexpression, prevents efficient virus release while ISG-15 knockdown does the opposite (Pincetic et al., 2010; Kuang et al., 2011). ISG-15 is being investigated as a potential target for novel antiretroviral drugs, and others have suggested ISG-15 as a biomarker for HAND progression (Skaug and Chen, 2010; Wang et al., 2012; Katsounas et al., 2013). Conversely, TSG-101 depletion reduces viral budding efficiency and is also being studied as a potential antiviral target (Pincetic et al., 2010; Kuang et al., 2011). Levels of ESCRT pathway, or associated, proteins may be predict HAND progression.

In this study we sought to determine if ISG-15, or ESCRT pathway machinery, levels correlate with HAND severity in postmortem frontal cortex brain tissue and cerebrospinal fluid (CSF). We hypothesized that brain and CSF ISG-15 levels would be increased during early stage HAND, and therefore, may predict progression to HIV-associated dementia (HAD) or other severe forms of HAND. Postmortem specimens from a large cohort of well-characterized HIV-infected patients were analyzed for frontal cortex and CSF levels of ISG-15, TSG-101, VPS-4 and LIP-5 by western blot, dot-blot, enzyme-linked immunosorbent assay (ELISA) and immunohistochemistry. Protein levels were then correlated to viral load and separated by HAND severity. Overall, our data indicate CSF ISG-15, LIP-5 and VPS-4 may indicate progressing HAND. Hence, ESCRT pathway, and

NIH-PA Author Manuscript

NIH-PA Author Manuscript

NIH-PA Author Manuscript

related, proteins, alone or in some combination, may potentially be useful to aid in diagnoses and treatment of HIV patients progressing to HAND.

Methods

Study population

For the present study we included a total of 47 HIV+ autopsy cases (Table 1) from the HIV Neurobehavioral Research Center and California Neuro Acquired Immunodeficiency Syndrome (AIDS) Tissue Network at the University of California, San Diego. Cases had neuromedical and neuropsychological examinations within a median of 12 months before death. Most cases died as a result of acute bronchopneumonia or septicemia and autopsy was performed within 24 hrs of death. Autopsy findings were consistent with AIDS and the associated pathology was most frequently due to systemic cytomegalovirus (CMV), Kaposi sarcoma, and liver disease. Subjects were excluded if they had a history of CNS opportunistic infections or non-HIV-related developmental, neurologic, psychiatric, or metabolic conditions that might affect CNS functioning (e.g., loss of consciousness exceeding 30 minutes, psychosis, substance dependence). The diagnosis of HIV encephalitis was based on the presence of microglial nodules, astrogliosis, HIV p24–positive cells, and myelin pallor.

Determination of HIV p24 levels in postmortem samples

HIV-1 p24 levels in postmortem tissues were determined using a commercially available p24 enzyme-linked immunosorbent assay (ELISA) (NEK050001KT, PerkinElmer, Waltham, MA). In brief, as previously described (Hashimoto et al., 2002), tissues from human brain samples (0.1 g) were homogenized in 0.7 mL of fractionation buffer containing phosphatase and protease inhibitor cocktails (Calbiochem, San Diego, CA). Samples were precleared by centrifugation at 5000 × g for 5 minutes at room temperature. Homogenate was analyzed for protein quantity by BCA assay (Thermo Scientific) and then 100 ug of sample was loaded onto a commercially available p24 enzyme-linked immunosorbent assay (ELISA; NEK050001KT, Perkin Elmer, Waltham, MA, USA) and performed according to the manufacturer’s protocol.

Antibodies

For western blot analysis, we used polyclonal antibodies against ISG-15 (200-401-438, dilution 1:250, Rockland), VPS-4 (sc-32922, dilution 1:500, Santa Cruz Biotechnology), and monoclonal antibodies against TSG-101 (612696, dilution 1:1000, BD Biosciences), LIP-5 (sc-374013, dilution 1:500, Santa Cruz Biotechnology) and actin (A5441, dilution 1:1000, Sigma).

Immunoblot analysis

Frontal cortex tissues from human brains were homogenized and fractionated using a buffer that facilitates separation of the membrane and cytosolic fractions (1.0 mmol/L HEPES, 5.0 mmol/L benzamidine, 2.0 mmol/L 2-mercaptoethanol, 3.0 mmol/L EDTA, 0.5 mmol/L magnesium sulfate, 0.05% sodium azide; final pH 8.8). In brief, as previously described, (Hashimoto et al., 2002) tissues from human brain samples (0.1 g) were homogenized in 0.7 mL of fractionation buffer containing phosphatase and protease inhibitor cocktails (Calbiochem, San Diego, CA). Samples were precleared by centrifugation at 5000 × g for 5 minutes at room temperature. Supernatants were retained and placed into appropriate ultracentrifuge tubes and were centrifuged at 436,000 × g for 1 hour at 4°C in a TL-100 rotor (Beckman Coulter, Brea, CA). This supernatant was collected, as representing the

NIH-PA Author Manuscript

NIH-PA Author Manuscript

NIH-PA Author Manuscript

cytosolic fraction, and the pellets were resuspended in 0.1 mL of buffer and rehomogenized for the membrane fraction.

After determination of the protein content of all samples by BCA Protein assay (Thermo Fisher Scientific, Rockford, IL), homogenates were loaded (20 μg total protein/lane), separated on 4–12% Bis-Tris gels and electrophoresed in 5% HEPES running buffer, and blotted onto Immobilon-P 0.45 μm membrane using NuPage transfer buffer. The membranes were blocked in either 5% nonfat milk/1% BSA in phosphate buffered saline (PBS) + 0.05% Tween-20 (PBST) or in 5% BSA in PBST for one hour. Membranes were incubated overnight at 4°C with primary antibodies. Following visualization, blots were stripped and probed with a mouse monoclonal antibody against Actin (1:2000, mab1501, Millipore, Billerica, MA) as a loading control. All blots were then washed in PBS, .05% tween-20 and then incubated with secondary species-specific antibodies (American Qualex, 1:5000 in BSA-PBST) and visualized with enhanced chemiluminescence reagent (ECL, Perkin-Elmer). Images were obtained and semi-quantitative analysis was performed with the VersaDoc gel imaging system and Quantity One software (Bio-Rad).

Immunohistochemistry and Image Analysis

Briefly, as previously described (Masliah et al., 2003), free-floating 40 μm thick vibratome sections were washed with Tris buffered saline (TBS, pH 7.4), pre-treated in 3% H_2O_2, and blocked with 10% serum (Vector Laboratories, Burlingame, CA), 3% bovine serum albumin (Sigma), and 0.2% gelatin in TBS-Tween (TBS-T). For human brains, sections from the midfronal cortex were used. Sections were incubated at 4 C overnight with the primary antibodies. Sections were then incubated in secondary antibody (1:75, Vector), followed by Avidin D-horseradish peroxidase (HRP, ABC Elite, Vector) and reacted with diaminobenzidine (DAB, 0.2 mg/ml) in 50 mM Tris (pH 7.4) with 0.001% H_2O_2. Control experiments consisted of incubation with pre-immune rabbit serum. Immunostained sections were imaged with a digital Olympus microscope and assessment of levels of ISG-15, TSG-101, VPS-4 and LIP-5 immunoreactivity was performed utilizing the Image- Pro Plus program (Media Cybernetics, Silver Spring, MD). For each case a total of three sections (10 images per section) were analyzed in order to estimate the average number of immunolabeled cells per unit area (mm^2) and the average intensity of the immunostaining (corrected optical density). In addition, double immunolabeling studies were performed as previously described (Spencer *et al*, 2009) to determine the cellular localization of the ESCRT markers. For this purpose, vibratome sections from the HIVE cases were immunostained with antibodies against the microclia marker Iba-1 (mouse monoclonal) or astroglia marker, glial fibrilary astrocytic protein (GFAP) and antibodies against either ISG-15, LIP-5, TSG-101 or VPS-4 (rabbit polyclonal). Sections were then reacted with secondary antibodies tagged with FITC to detect Iba-1 and GFAP and with the tyramide Red amplification system (Perkin-Elmer) to detect ESCRT markers. Sections were mounted on superfrost slides (Fisher) and coverslipped with media containing DAPI. Sections were imaged with a Zeiss 63X (N.A. 1.4) objective on an Axiovert 35 microscope (Zeiss, Germany) with an attached MRC1024 laser scanning confocal microscope system (BioRad, Hercules, CA).

Statistical analysis

All the analyses were conducted on blind-coded samples. After the results were obtained, the code was broken and data were analyzed with the StatView program (SAS Institute, Inc., Cary, NC). Comparisons among groups were performed with one-way ANOVA with posthoc Fisher test, unpaired Student's T test and Chi square analysis. Correlation coefficients were calculated using linear regression analysis or stepwise regression analysis. Stepwise regression analysis was applied to the aggregated ESCRT protein expression data

NIH-PA Author Manuscript

NIH-PA Author Manuscript

NIH-PA Author Manuscript

to determine which proteins may contribute to statistically significant model for predicting HAND severity. All results were expressed as mean ±SEM. The differences were considered to be significant if p values were <0.05.

Role of the funding source

The funding source had no role in the study design, data collection, data analysis, data interpretation or writing of this report. The corresponding author had full access to all the data and had final responsibility for the decision to submit the paper for publication.

Results

Clinical characteristics of HIV+ donors

Before analyzing ESCRT pathway protein (ISG-15, TSG-101, VPS-4, LIP-5) levels, we first meticulously collected and characterized clinical and neuropathological aspects of the postmortem HIV+ cohort. For this purpose, at first, a total of 47 autopsy cases, with CSF available, were analyzed (normal, n=8; NPI/NPI-O, n=19; MCMD, n=13; HAD, n=7). In order to assess relevant differences between postmortem brain samples from patients with varying degrees of HAND, we characterized the cohorts by brain pathology, CD4+ cell count, viral load, and neuropsychological impairment status. The cohort was grouped by neurocognitive assessment and was predominantly male (89%) (Table 1). Eight (17%) of the cases were diagnosed as normal, nineteen (40%) as NPI/NPI-O, 13 (28%) as MCMD and seven (15%) as HAD. (Table 1). Brain weight varied from 1429 g for normal to a mean of 1283 g for HAD specimens (Table 1).

In Table 2 the cohort grouped by neurocognitive assessment and neuropahtological diagnoses. Interestingly, 4/8 patients (50%) with normal neurocognitive assessment showed HIVE pathology, while two (25%) were normal, one (13%) PML and one (13%) as other. Four (21%) of NPI/NPI-O group showed normal pathology, one (5%) MNE, three (16%) PML, five (26%) HIVE and six (32%) as other (Table 2). Four (31%) of the MCMD group had normal brain pathology, four (31%) MNE, one (8%) HIVE and four (31%) as other. The HAD group had no normal pathology diagnoses, however, one (14%) patient had MNE, one (14%) PML, four (57%) had HIVE and one (14%) other (Table 2). All 8 of the patients classified as normal had history of ARV, while four of 19 from the NPI/NPI-O group were ARV naïve. One of the MCMD group and three of the eight in the HAD group also no ARV history. These data indicate stark differences in the pathology among variable neuropsychological states in this HIV+ cohort.

CSF ESCRT protein levels; increased ISG-15, VPS-4 and LIP-5 CSF levels in patients with varying degrees of neuropsychological impairment

Retroviruses employ host cells ESCRT machinery to facilitate viral budding. In order to determine if ESCRT protein levels are good candidate biomarkers for early stage HAND we analyzed CSF from HIV+ patients with neuropsychological ratings of normal, NPI/NPI-O, MCMD and HAD. ELISA (ISG-15) or dot-blot (TSG-101, VPS-4 and LIP-5) were used to ascertain CSF ISG-15, TSG-101, VPS-4 and LIP-5 levels (Figure 1). CSF ISG-15 levels are increased 7-fold compared to normal in the NPI/NPI-O group, and 5- and 4-fold in the MCMD and HAD groups, respectively (Figure 1A). CSF ISG-15 levels as grouped by neuropathological diagnoses showed MNE ISG-15 was 3-fold higher than normal, while PML and other were increased 1.5- and 3-fold, respectively (Figure 1B). Interestingly, ISG-15 levels were increased 4.5-fold ($p<0.05$) over patients with normal pathology. CSF TSG-101 levels were analyzed by dotblot are essentially unchanged among the HIV+ cohort when classified by neurocognitive assessment (Figure 1C). Compared to normal cases, CSF TSG-101 levels were increased 1.6-, 1.5- and 1.5-fold in PML, HIVE and other cases,

NIH-PA Author Manuscript

NIH-PA Author Manuscript

NIH-PA Author Manuscript

respectively (Figure 1D). CSF VPS-4 levels are significantly ($p<0.05$) increased by 2-fold in NPI/NPI-O specimens compared to normal, and 1.5- and 3-fold compared to MCMD and HAD specimens, respectively (Figure 1E). VPS-4 CSF levels are unchanged in MNE and PML patients compared to normal; however, HIVE and other mean VPS-4 levels are increased compared to normal (Figure 1F). LIP-5 levels are unchanged in NOI/NPI-O and MCMD compared to normal, but LIP-5 levels are increased 1.8-fold in HAD compared to normal cases (Figure 1G). LIP-5 CSF levels were elevated in all patients with some neuropathological diagnoses compared to normal (Figure 1H). LIP-5 CSF levels in patients diagnosed as other pathology were significantly ($p<0.05$) increased compared to normal cases. Comparisons among groups were performed with one-way ANOVA with posthoc Fisher test and stepwise linear regression modeling.

Elevated ISG-15 in HIVE CSF and concomitant increased CSF LIP-5 expression

Cells evolved an innate mechanism to block viral replication by inhibiting proper ESCRT function in the presence of invading virus. To determine ISG-15's potential as an informative biomarker for predicting increased chance for developing HAND we further analyzed ISG-15 and LIP-5 CSF levels. MNE, PML, HIVE and Other groups each have a higher percentage of donors over the mean when compared to the normal cohort. Interestingly, the HIVE group had the highest (75 %) percentage of donors with CSF ISG-15 levels over the mean (Figure 2A). Upon more in depth analyses we found that CSF LIP-5 levels are significantly ($p<0.05$) higher in CSF samples with above mean ISG-15 levels (Figure 2B). Groups were compared using unpaired Student's T test and Chi square analysis (Figure 2B). CSF ISG-15 positively correlates ($p<0.01$) with LIP-5 levels in HIV+ patients (Figure 2C). These data suggest that ISG-15 and LIP-5 may indicate more severe neurocognitive impairment/pathology. Correlation coefficients were calculated using linear regression analysis (Figure 2C).

Increased CNS viral burden coincides with more severe HAND and increased ISG-15 levels

HIV enters the brain early on during infection; however, for unknown reasons, not all HIV patients develop HAND. To determine if viral burden was indicative of HAND severity in our cohort, we analyzed HIV RNA and/or p24 capsid protein levels in CSF and brain, and according mean ISG-15 levels. HIV RNA levels are unchanged among different neurocognitive assessment groups, with a 1.3-fold increase in the HAD group compared to the normal group (Figure 3A). HIV RNA levels are increased in all neuropathological groups compared to normal, and importantly, HIV RNA in HIVE group is significantly ($p<0.01$) increased compared to the normal group (Figure 3B). Brain p24 levels are significantly ($p<0.05$) increased in HAD specimens compared to NPI/NPI-O and MCMD groups, but not to normal (Figure 3C). However, brain p24 levels are unchanged among neuropathological groupings, except in HIVE cases; p24 in HIVE cases is significantly (12-fold; $p<0.05$) increased compared to normal cases (Figure 3D). Comparisons among groups were performed with one-way ANOVA with posthoc Fisher test (Figures 3A–D). CSF HIV RNA positively correlates ($p<0.0002$) with brain p24 levels (Figure 3E). Correlation coefficients were calculated using linear regression analysis (Figure 3E). HIV p24 levels are significantly ($p<0.001$; 11-fold) increased in CSF of donors with above the mean ISG-15 levels compared to those below the mean (Figure 3G). These findings may indicate that, in this cohort, increased CNS viral burden coexists with increased neurocognitive assessment, neuropathological diagnoses and CSF ISG-15 levels. Groups were compared using unpaired Student's T test and Chi square analysis (Figure 3G).

NIH-PA Author Manuscript

NIH-PA Author Manuscript

NIH-PA Author Manuscript

ESCRT protein levels increase in brain tissues from donors with more severe neuropathological diagnoses

HIV uses the ESCRT system to facilitate viral replication. To determine if ESCRT protein levels are increased in the CNS during HIV infection we analyzed ISG-15, TSG-101, VPS-4 and LIP-5 levels in brain tissue by immunoblot. ISG-15 signal are clearly of increased intensity in MNE, PML and HIVE cases compared to normal cases (Figure 4A). Similarly, the bands corresponding to TSG-101 are elevated in MNE, PML and HIVE compared to normal cases (Figure 4A). Densitometry analyses of ISG-15 bands normalized to actin, and while MNE and PML are increased, HIVE ISG-15 density is significantly ($p<0.05$) increased compared to normal cases (Figure 4B). Brain TSG-101 levels are increased in MNE, PML and HIVE cases, but significantly ($p<0.05$) in the latter two groups compared to normal cases (Figure 4C). VPS-4 signal is low in all but one case from the normal group; however, levels trend higher in MNE, PML and HIVE groups (Figure 4D). LIP-5 immunoblot clearly shows increased LIP-5 band intensity in MNE, PML and HIVE cases compared to normal (Figure 4D). VPS-4 densitometry is increased in MNE, PML and HIVE groups compared to normal, but levels are most intense in the PML group (Figure 4E). LIP-5 densitometry is most intense ($p<0.01$) in MNE compared to normal cases, but LIP-5 levels are also increased PML and HIVE compared to normal (Figure 4F). These data suggest that brain ESCRT protein levels are increased with increased HIV neuropathology. In order to determine if clustering the ESCRT marker expression data added to the significance of the correlation, stepwise regression analysis was performed. Comparisons among groups were performed with one-way ANOVA with posthoc Fisher test and stepwise linear regression modeling. This study using immunoblot data of ESCRT proteins generated a statistical model for predicting neuropathology based on protein expression levels (Table 3). Results show statistical significance ($p<0.013$, R Square = 0.625) for predicting neuropathology severity (Tables 3–5). In summary, TSG-101 was the strongest predictor, followed by VPS-4, ISG-15 and LIP-5.

ESCRT protein immunoreactivity is increased in brains of HIV+ and HIVE compared to uninfected patients

HIV infects CD4+ cells, represented by microglia in the CNS. Neurons and astrocytes are less suitable to infection, but may be affected by infection and inflammation as bystanders. Furthermore, HIV proteins that influence ESCRT machinery expression may enter these bystander cells. To determine brain ESCRT proteins are increased in HIV+ brain, and the cellular expression patterns, we immunostained brain frontal cortex from control, HIV+ and HIVE donors with ISG-15, TSG-101, VPS-4 and LIP-5 antibodies. ISG-15 levels in HIV+ patients are increased compared to control. ISG-15 immunostaining is most intense in HIVE cases. Furthermore, ISG-15 appears detectable in glial cells (top) and neurons (bottom) (Figure 5A). ISG-15 optical density is significantly ($p<0.05$) increased in HIV+ and HIVE brains compared to control (Figure 5B). LIP-5 immunostaining is increased in HIV+ and HIVE compared to control cases; immunostaining appears to be most intense in HIVE brains (Figure 5C). LIP-5 optical density is significantly increased in HIVE compared to control (Figure 5D). TSG-101 immunostaining is most intense in HIVE cases compared to control or HIV+ cases (Figure 5E). TSG-101 optical intensity is increased in HIV+ and HIVE compared to control; however the differences are not significant (Figure 5F). VPS-4 immunostaining is increased in HIV+ and HIVE compared to control cases, and most intense in HIVE brains (Figure 5G). VPS-4 optical density is significantly increased in HIVE compared to control (Figure 5H). These data support earlier findings that CNS HIV infection may increase glial and neuronal ESCRT protein expression. Comparisons among groups were performed with one-way ANOVA with posthoc Fisher test.

NIH-PA Author Manuscript

NIH-PA Author Manuscript

NIH-PA Author Manuscript

ESCRT protein immunoreactivity in microglia and astrocyte cells in HIVE brains

HIV-1 infects microglia and, to a lesser extent, astrocytes. Infected microglia secrete inf and other cytokines which activate uninfected microglia and astrocytes. To determine glial ESCRT protein expression during HIVE we immunostained brain frontal cortex from HIVE donors with ISG-15, LIP-5, TSG-101 and VPS4 antibodies alone or in conjunction with Iba-1 (microglia) or GFAP (astrocytes) antibodies. ISG-15, LIP-5, TSG-101 and VPS-4 (red) each colocalized with Iba-1 (green) in HIVE brains (Figure 6A). TSG-101 and VPS-4 immunostaining appear to produce the strongest signal with Iba-1 colocalization (yellow) (Figure 6A). ISG-15, LIP-5, TSG-101 and VPS-4 (red) also colocalized with GFAP (green) immunostaining for astrocytes (Figure 6B). These data illustrate ESCRT and related proteins are expressed in microglia and astrocytes during HIVE.

Discussion

In the current report we present findings from a comprehensive analysis of ESCRT pathway, and related, protein (ISG-15, VPS-4, TSG-101 and LIP-5) expression in the CSF and brains of HIV infected individuals suffering from a range of HAND. Overall, increased CSF levels of ISG-15, VPS-4 and LIP-5 may indicate early stage HAND and therefore be predictive of future neurocognitive impairments. The 47-patient cohort of HIV+ donors runs the gamut from normal cognitive assessment to HAD, and from no pathology to HIVE. CSF ISG-15 and VPS-4 are elevated during early stages of neurocognitive impairment and levels are reduced in HAD CSF. Brain tissues show increased levels of all ESCRT proteins in brains with more severe neuropathology. Viral load is highest in HIVE donors, as expected, but the p24 level correlation with less severe pathologies is not linear. Previous studies suggest that ISG-15 may be a predictive biomarker for HAND (Wang et al., 2012; Katsounas et al., 2013); however, CSF VPS-4 levels may be a more dependable predictor of early HAND. Furthermore, LIP-5 levels may indicate more progressed HAND when levels correlate with ISG-15. These data are synchronous with previous findings that show HIV highjacks the ESCRT system and ISG-15 is upregulated to combat virus infiltration (Grover et al., 2013). This study suggests the ESCRT pathway machinery CSF levels may provide insight into HAND progression, and in concert with other tools, may aid physicians in prescribing appropriate therapy.

The present study was spurred by mounting literature indicating the ESCRT pathway is integral in establishing, and maintaining, HIV infection (Langelier et al., 2006; Wang et al., 2012; Grover et al., 2013); however these data represent the first comprehensive survey of a well characterized cohort of HIV+ patients. Normally, cells employ ESCRT pathway proteins (TSG-101, VPS-4, LIP-5, etc.) to facilitate membrane fission during multivesicular body formation and cytokinesis (Jouvenet, 2012). HIV uses the ESCRT system to facilitate viral budding through the plasma membrane into the extracellular space where the virus can infect bystander cells (Pincetic et al., 2010; Kuang et al., 2011). Virus infection induces interferon release from infected cells, which in-turn stimulates ISG-15 expression, along with other antiviral mechanisms. Figure 6 illustrates the ESCRT pathway and how ISG-15 expression prevents efficient viral budding. ISG-15 is conjugated to ESCRT pathway proteins to prevent proper viral budding. The known steps through which ISG-15 combats viral replication include: **1)** ISG-15 is conjugated to CHMP5 thereby preventing LIP-5:CHMP5 association and subsequent localization to the plasma membrane. **2)** Lack of LIP-5:CHMP5 at the plasma membrane prevents VPS-4 associating with its coactivator, LIP-5 and ATPase activity that is essential for virus release. **3)** CHMP2A is ISGylated in the presence of CHMP5:ISG-15, which prevents CHMP2A binding to LIP-5 and VPS-4. **4)** CHMP6 is ISGylated thereby weakening association with VPS-4. **5)** Unbound VPS-4 is released to the cytosol, and viral budding is inhibited. **6)** ISG15 expression prevents TSG101

NIH-PA Author Manuscript

NIH-PA Author Manuscript

NIH-PA Author Manuscript

interaction with GAG, and thereby prevents viral budding. (Langelier et al., 2006; Pincetic et al., 2010; Kuang et al., 2011; Wang et al., 2012). Recently it was reported that ISG-15 is highly expressed in animal models for global ischemia, traumatic brain injury and gp120 expression in the cortex (Nakka et al., 2011; Wang et al., 2012). Moreover, high baseline ISG-15 levels and reduced responsiveness to ifn-α are strong indicators of negative therapeutic response in patients co-infected with HIV-HCV (Katsounas et al., 2013). Whether ISG-15 brain levels are indicative of future HAND is unknown. Here, we began by surveying a 47-patient cohort for CSF and brain frontal cortex levels of ISG-15. Our ISG-15 analysis in human brain samples proved to be consistent with reports that show increased ISG-15 expression in mouse models for HIV-induced brain injury (Wang et al., 2012). CSF levels in this cohort suggest ISG-15 may be elevated during early stage HAND before subsiding to less elevated levels during HAD. These high ISG-15 levels at beginning stages of HAND may represent a strong innate response to HIV infiltration of the CNS. Our data suggest ISG-15 levels are elevated, but off their peak, during HAD. Interestingly, CSF ISG-15 was highest in brains HIVE neuropathology, and ISG-15 levels positively correlate to LIP-5 levels in the same samples, discussed later. One hurdle is to establish a baseline ISG-15 CSF level for HIV+ patients, rather it be related to another marker or in conjunction with viral load or CD4+ cell count. Immunohistochemistry for ISG-15 in control, HIV+ and HIVE brains reflected findings from the gp120 mouse model, and suggest HIV induces ISG-15 expression in the brain; importantly, expression appears not to be isolated to microglia, but also presumably uninfected neurons. This aberrant gene expression may represent the sort of mechanism that confounds normal neuronal function during HAND. Presumably, HIV-1 infection-induced ifn stimulates infected and uninfected glia and neurons to increase ISG15 expression. HIV-1 or viral proteins may contribute to increased ESCRT protein expression in bystander cells leading to cellular dysfunction associated with HAND. Therefore, therapies targeted to block HIV protein activity or inflammation may be useful. Overall there were some discrepancies in the robustness of ISG-15 expression between the mouse studies and the postmortem tissues; this may be attributed to organism complexity or innate antiviral pathway specific differences between the species (Wang et al., 2012).

Next, we hypothesized that ESCRT machinery proteins, which are directly involved in HIV budding, may be overexpressed in the brain and CSF during HIV infection. Light has been shed on HIV utilizing the ESCRT system to facilitate viral budding, and how ISG-15 combats this mechanism (Figure 6) (Pincetic et al., 2010; Kuang et al., 2011). TSG-101 is an ESCRT pathway protein that recognizes and sorts ubiquitinated proteins for assimilation to vacuoles (Li et al., 1999; Babst et al., 2000; Dupre et al., 2001). It has recently been reported that TSG-101 facilitates HIV budding by binding to HIV GAG (VerPlank et al., 2001; Demirov et al., 2002; Chen and Liu, 2008). VPS-4 is a cytosolic protein that is recruited to the membrane-bound ESCRT complex (Jouvenet, 2012). VPS-4 dimers co-assemble into a double hexameric ring with coactivator LIP-5 (Shim et al., 2008). ATP hydrolysis by the VPS-4:LIP-5 oligomer simultaneously releases the ESCRT complex to the cytoplasm and the virus to the extracellular milieu (Ward et al., 2005). ISG-15 conjugation to CHMP5 prevents this VPS-4:LIP-5 interaction (Figure 6) (Pincetic et al., 2010; Kuang et al., 2011). In these studies TSG-101 expression does not appear to be a predictive marker of HAND progression; however, VPS-4 and/or LIP-5 may be promising biomarkers for predicting HAND. Interestingly, CSF VPS-4 levels showed the most promise for indicating early stage HAND. Again, establishing a baseline VPS-4 level will be a challenge, but elevated VPS-4 may indicate early stages of HAND as CSF VPS-4 levels were decreased in later stages of HAND. CSF LIP-5 correlation with ISG-15 may provide a useful co-marker to corroborate evidence that the antiviral response is active in the brain. Taken together these data suggest HIV may regulate LIP-5 and VPS-4 expression to combat ISGylation and facilitate virus release. Hence VPS-4 and LIP-5 may be used in concert with other markers to identify

NIH-PA Author Manuscript

NIH-PA Author Manuscript

NIH-PA Author Manuscript

patient in pre-dementia stages of HIV infection. However, brain immunostaining for VPS-4 and LIP-5 suggests these proteins remain highly expressed throughout HAD. It is noteworthy that high ISG-15 CSF levels may indicate severe neuropathology when levels positively correlate to CSF LIP-5 levels. Establishing a standard high:low ISG-15 level in the CSF of HIV patients could aid diagnosis and ART prescription, and CSF LIP-5 levels may support or diminish the diagnosis. Interestingly, more in-depth statistical analysis (linear stepwise regression modeling) of ISG15, TSG101, VPS4 and LIP5 in aggregate shows CSF levels are not indicative of HAND severity; however, tissue protein expression data provide a statistically significant model for predicting neuropathology severity. A longintudinal study using patient CSF may prove efficacious in establishing, or ruling out, these proteins as HAND biomarkers. It is noteworthy that all of the patients that tested normal on psychological tests had history of ARV regimen, while that was not the case for the other three psychological classifications. Taken together, these data show CSF ISG-15, VPS-4, LIP-5, HIV RNA or brain protein levels indicated more progressed HAND and more severe neuropathology.

The HIV-infected population is rapidly aging and these patients are particularly susceptible to developing premature neurocognitive disorders. Biomarkers that could give clinicians a head start to combat HAND will be valuable as they prescribe ART. These studies provide a CNS survey of a very popular family of proteins intricately involved in HIV budding. Herein we identify ISG-15, VPS-4, TSG-101 and LIP-5 levels as potential promising biomarkers for predicting HIV neuropathology and HAND.

Acknowledgments

We thank the National Institutes of Aging (AG043384), the National Institutes of Mental Health (MH062962, MH5974 and MH83506) and the National Institute for Neurological Disorders and Stroke (1F32NS083426-01) funding this work.

Bibliography

HIV/AIDS surveillance report. 2007. p. 1-54.

Babst M, Odorizzi G, Estepa EJ, Emr SD. Mammalian tumor susceptibility gene 101 (TSG101) and the yeast homologue, Vps23p, both function in late endosomal trafficking. Traffic. 2000; 1:248–258. [PubMed: 11208108]

Budka H, Costanzi G, Cristina S, Lechi A, Parravicini C, Trabattoni R, Vago L. Brain pathology induced by infection with the human immunodeficiency virus (HIV). A histological, immunocytochemical, and electron microscopical study of 100 autopsy cases. Acta Neuropathol(Berl). 1987; 75:185–198. [PubMed: 3434225]

Chen HF, Liu XY. [The action of TSG101 on HIV-1 budding and related inhibitors]. Yao xue xue bao = Acta pharmaceutica Sinica. 2008; 43:1165–1170. [PubMed: 19244744]

Cherner M, Cysique L, Heaton RK, Marcotte TD, Ellis RJ, Masliah E, Grant I. Neuropathologic confirmation of definitional criteria for human immunodeficiency virus-associated neurocognitive disorders. J Neurovirol. 2007; 13:23–28. [PubMed: 17454445]

Demirov DG, Ono A, Orenstein JM, Freed EO. Overexpression of the N-terminal domain of TSG101 inhibits HIV-1 budding by blocking late domain function. Proc Natl Acad Sci U S A. 2002; 99:955–960. [PubMed: 11805336]

Dupre S, Volland C, Haguenauer-Tsapis R. Membrane transport: ubiquitylation in endosomal sorting. Curr Biol. 2001; 11:R932–R934. [PubMed: 11719242]

Everall I, Salaria S, Roberts E, Corbeil J, Sasik R, Fox H, Grant I, Masliah E. Methamphetamine stimulates interferon inducible genes in HIV infected brain. J Neuroimmunol. 2005; 170:158–171. [PubMed: 16249037]

Gelman BB, Chen T, Lisinicchia JG, Soukup VM, Carmical JR, Starkey JM, Masliah E, Commins DL, Brandt D, Grant I, Singer EJ, Levine AJ, Miller J, Winkler JM, Fox HS, Luxon BA, Morgello S.

NIH-PA Author Manuscript

NIH-PA Author Manuscript

NIH-PA Author Manuscript

The National NeuroAIDS Tissue Consortium brain gene array: two types of HIV-associated neurocognitive impairment. PLoS One. 2012; 7:e46178. [PubMed: 23049970]

Gendelman H, Lipton S, Tardieu M, Bukrinsky M, Nottet H. The neuropathogenesis of HIV-1 infection. JLeukocyte Biol. 1994; 56:389–398. [PubMed: 8083614]

Gerena Y, Skolasky RL, Velez JM, Toro-Nieves D, Mayo R, Nath A, Wojna V. Soluble and cell-associated insulin receptor dysfunction correlates with severity of HAND in HIV-infected women. PLoS One. 2012; 7:e37358. [PubMed: 22629383]

Grover JR, Llewellyn GN, Soheilian F, Nagashima K, Veatch SL, Ono A. Roles played by capsid-dependent induction of membrane curvature and Gag-ESCRT interactions in tetherin recruitment to HIV-1 assembly sites. J Virol. 2013; 87:4650–4664. [PubMed: 23408603]

Hashimoto M, Sagara Y, Everall IP, Mallory M, Everson A, Langford D, Masliah E. Fibroblast growth factor 1 regulates signaling via the GSK3{beta} pathway: implications for neuroprotection. J Biol Chem. 2002; 277:32985–32991. [PubMed: 12095987]

Havlir DV, Currier JS. Complications of HIV disease and antiretroviral therapy. Topics in HIV medicine : a publication of the International AIDS Society, USA. 2006; 14:27–35.

Heaton RK, Cysique LA, Jin H, Shi C, Yu X, Letendre S, Franklin DR, Ake C, Vigil O, Atkinson JH, Marcotte TD, Grant I, Wu Z. Neurobehavioral effects of human immunodeficiency virus infection among former plasma donors in rural China. J Neurovirol. 2008; 14:536–549. [PubMed: 18991068]

Heaton RK, et al. HIV-associated neurocognitive disorders persist in the era of potent antiretroviral therapy: CHARTER Study. Neurology. 2010; 75:2087–2096. [PubMed: 21135382]

Heaton RK, et al. HIV-associated neurocognitive disorders before and during the era of combination antiretroviral therapy: differences in rates, nature, and predictors. J Neurovirol. 2011; 17:3–16. [PubMed: 21174240]

Joska JA, Gouse H, Paul RH, Stein DJ, Flisher AJ. Does highly active antiretroviral therapy improve neurocognitive function? A systematic review. J Neurovirol. 2010; 16:101–114. [PubMed: 20345318]

Jouvenet N. Dynamics of ESCRT proteins. Cell Mol Life Sci. 2012; 69:4121–4133. [PubMed: 22669260]

Katsounas A, Hubbard JJ, Wang CH, Zhang X, Dou D, Shivakumar B, Winter S, Schlaak JF, Lempicki RA, Masur H, Polis M, Kottilil S, Osinusi A. High interferon-stimulated gene ISG-15 expression affects HCV treatment outcome in patients co-infected with HIV and HCV. J Med Virol. 2013; 85:959–963. [PubMed: 23588721]

Kuang Z, Seo EJ, Leis J. Mechanism of inhibition of retrovirus release from cells by interferon-induced gene ISG15. J Virol. 2011; 85:7153–7161. [PubMed: 21543490]

Langelier C, von Schwedler UK, Fisher RD, De Domenico I, White PL, Hill CP, Kaplan J, Ward D, Sundquist WI. Human ESCRT-II complex and its role in human immunodeficiency virus type 1 release. J Virol. 2006; 80:9465–9480. [PubMed: 16973552]

Li Y, Kane T, Tipper C, Spatrick P, Jenness DD. Yeast mutants affecting possible quality control of plasma membrane proteins. Mol Cell Biol. 1999; 19:3588–3599. [PubMed: 10207082]

Lichtfuss GF, Hoy J, Rajasuriar R, Kramski M, Crowe SM, Lewin SR. Biomarkers of immune dysfunction following combination antiretroviral therapy for HIV infection. Biomarkers in medicine. 2011; 5:171–186. [PubMed: 21473720]

Masliah E, Alford M, Adame A, Rockenstein E, Galasko D, Salmon D, Hansen LA, Thal LJ. Abeta1–42 promotes cholinergic sprouting in patients with AD and Lewy body variant of AD. Neurology. 2003; 61:206–211. [PubMed: 12874400]

Merino JJ, Montes ML, Blanco A, Bustos MJ, Oreja-Guevara C, Bayon C, Cuadrado A, Lubrini G, Cambron I, Munoz A, Cebolla S, Gutierrez-Fernandez M, Bernardino JI, Arribas JR, Fiala M. [HIV-1 neuropathogenesis: therapeutic strategies against neuronal loss induced by gp120/Tat glycoprotein in the central nervous system]. Revista de neurologia. 2011; 52:101–111. [PubMed: 21271550]

Montaner JS, Cote HC, Harris M, Hogg RS, Yip B, Chan JW, Harrigan PR, O'Shaughnessy MV. Mitochondrial toxicity in the era of HAART: evaluating venous lactate and peripheral blood

NIH-PA Author Manuscript

NIH-PA Author Manuscript

NIH-PA Author Manuscript

mitochondrial DNA in HIV-infected patients taking antiretroviral therapy. J Acquir Immune Defic Syndr. 2003; 34(Suppl 1):S85–S90. [PubMed: 14562863]

Nakka VP, Lang BT, Lenschow DJ, Zhang DE, Dempsey RJ, Vemuganti R. Increased cerebral protein ISGylation after focal ischemia is neuroprotective. J Cereb Blood Flow Metab. 2011; 31:2375–2384. [PubMed: 21847135]

Okumura A, Lu G, Pitha-Rowe I, Pitha PM. Innate antiviral response targets HIV-1 release by the induction of ubiquitin-like protein ISG15. Proc Natl Acad Sci U S A. 2006; 103:1440–1445. [PubMed: 16434471]

Pendyala G, Want EJ, Webb W, Siuzdak G, Fox HS. Biomarkers for neuroAIDS: the widening scope of metabolomics. J Neuroimmune Pharmacol. 2007; 2:72–80. [PubMed: 18040828]

Pincetic A, Kuang Z, Seo EJ, Leis J. The interferon-induced gene ISG15 blocks retrovirus release from cells late in the budding process. J Virol. 2010; 84:4725–4736. [PubMed: 20164219]

Poteet E, Choudhury GR, Winters A, Li W, Ryou MG, Liu R, Tang L, Ghorpade A, Wen Y, Yuan F, Keir ST, Yan H, Bigner DD, Simpkins JW, Yang SH. Reversing the Warburg effect as a treatment for glioblastoma. J Biol Chem. 2013; 288:9153–9164. [PubMed: 23408428]

Sharma TS, Jacobson D, Anderson LM, Gerschenson M, Vandyke R, McFarland E, Miller T. The Relationship between Mitochondrial Dysfunction and Insulin Resistance in HIV-infected Children Receiving Antiretroviral Therapy. AIDS Res Hum Retroviruses. 2013

Shim S, Merrill SA, Hanson PI. Novel interactions of ESCRT-III with LIP5 and VPS4 and their implications for ESCRT-III disassembly. Mol Biol Cell. 2008; 19:2661–2672. [PubMed: 18385515]

Skaug B, Chen ZJ. Emerging role of ISG15 in antiviral immunity. Cell. 2010; 143:187–190. [PubMed: 20946978]

Strathdee SA, O'Shaughnessy MV, Montaner JS, Schechter MT. A decade of research on the natural history of HIV infection: Part 1. Markers. Clinical and investigative medicine Medecine clinique et experimentale. 1996; 19:111–120. [PubMed: 8697670]

VerPlank L, Bouamr F, LaGrassa TJ, Agresta B, Kikonyogo A, Leis J, Carter CA. Tsg101, a homologue of ubiquitin-conjugating (E2) enzymes, binds the L domain in HIV type 1 Pr55(Gag). Proc Natl Acad Sci U S A. 2001; 98:7724–7729. [PubMed: 11427703]

Wang RG, Kaul M, Zhang DX. Interferon-stimulated gene 15 as a general marker for acute and chronic neuronal injuries. Sheng li xue bao : [Acta physiologica Sinica]. 2012; 64:577–583.

Ward DM, Vaughn MB, Shiflett SL, White PL, Pollock AL, Hill J, Schnegelberger R, Sundquist WI, Kaplan J. The role of LIP5 and CHMP5 in multivesicular body formation and HIV-1 budding in mammalian cells. J Biol Chem. 2005; 280:10548–10555. [PubMed: 15644320]

NIH-PA Author Manuscript
NIH-PA Author Manuscript
NIH-PA Author Manuscript

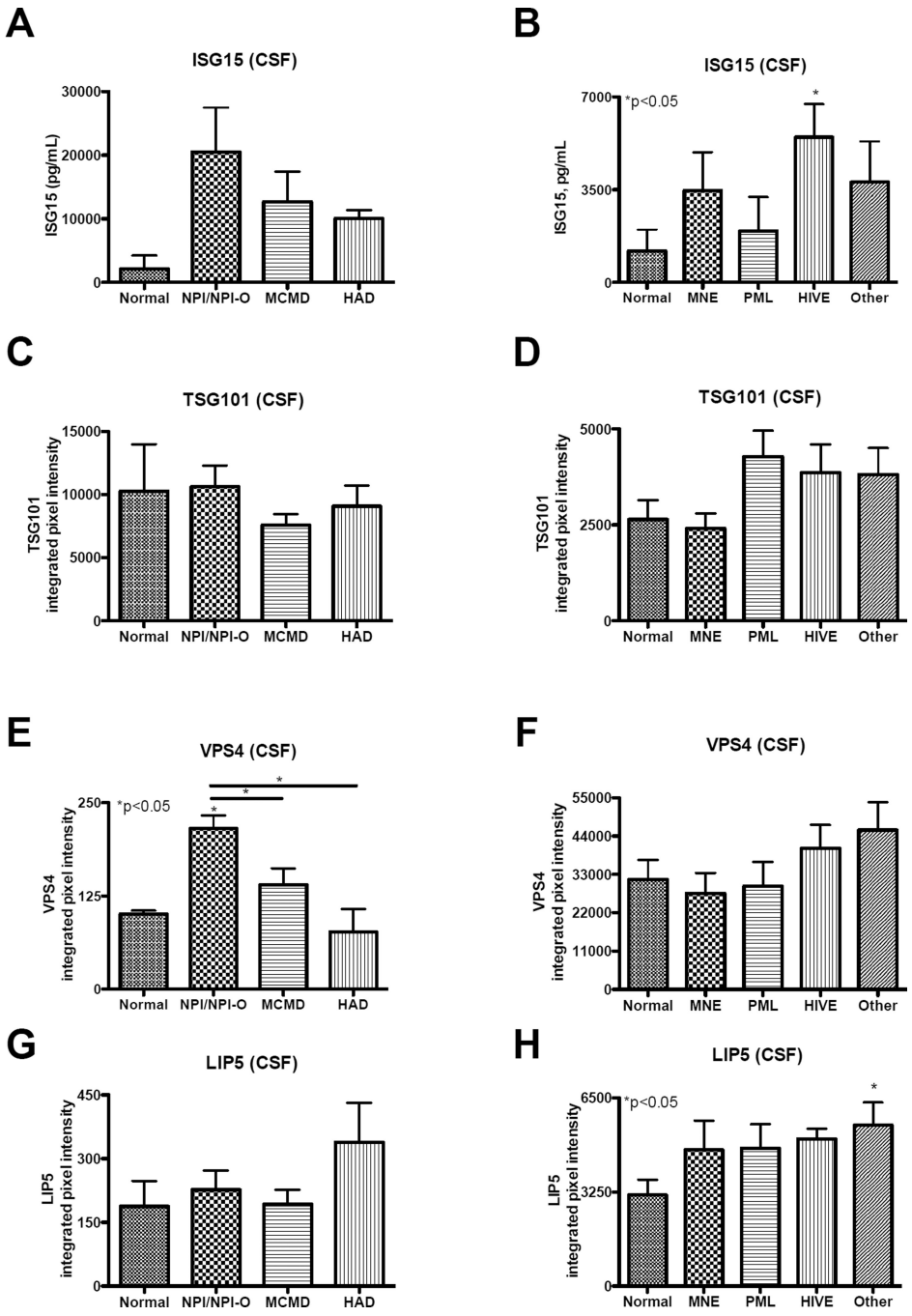

Fig. 1. CSF ESCRT protein levels; increased ISG-15, VPS-4 and LIP-5 CSF levels in patients with varying degrees of neuropsychological impairment

A. CSF ISG-15 levels as measured by ELISA and grouped by neurocognitive assessment. **B.** CSF ISG-15 levels as measured by ELISA and grouped by neuropathological diagnosis. **C.** CSF TSG-101 levels as measured by dot-blot and grouped by neurocognitive assessment. **D.** CSF TSG-101 levels as measured by ELISA and grouped by neuropathological diagnosis. **E.** CSF VPS-4 levels as measured by dot-blot and grouped by neurocognitive assessment. **F.** CSF VPS-4 levels as measured by ELISA and grouped by neuropathological diagnosis. **G.** CSF LIP-5 levels as measured by dot-blot and grouped by neurocognitive assessment. **H.** CSF LIP-5 levels as measured by ELISA and grouped by neuropathological diagnosis. For

NIH-PA Author Manuscript

NIH-PA Author Manuscript

NIH-PA Author Manuscript

statistics, CSF from a total of n= 24 cases was categorized by neurocognitive impairment, of them n= 5 normal, n= 9 NPI/NPI-O, n= 9 MCMD, n= 3 HAD. CSF from a total of n= 35 postmortem cases were categorized by neuropathological assessment: n= 9 normal, n=6 MNE, n= 4 PML, n= 8 HIVE, n= 8 other. Statistical significance (*$p<0.05$, One-way ANOVA, post hoc Fisher test) compared to normal.

NIH-PA Author Manuscript

NIH-PA Author Manuscript

NIH-PA Author Manuscript

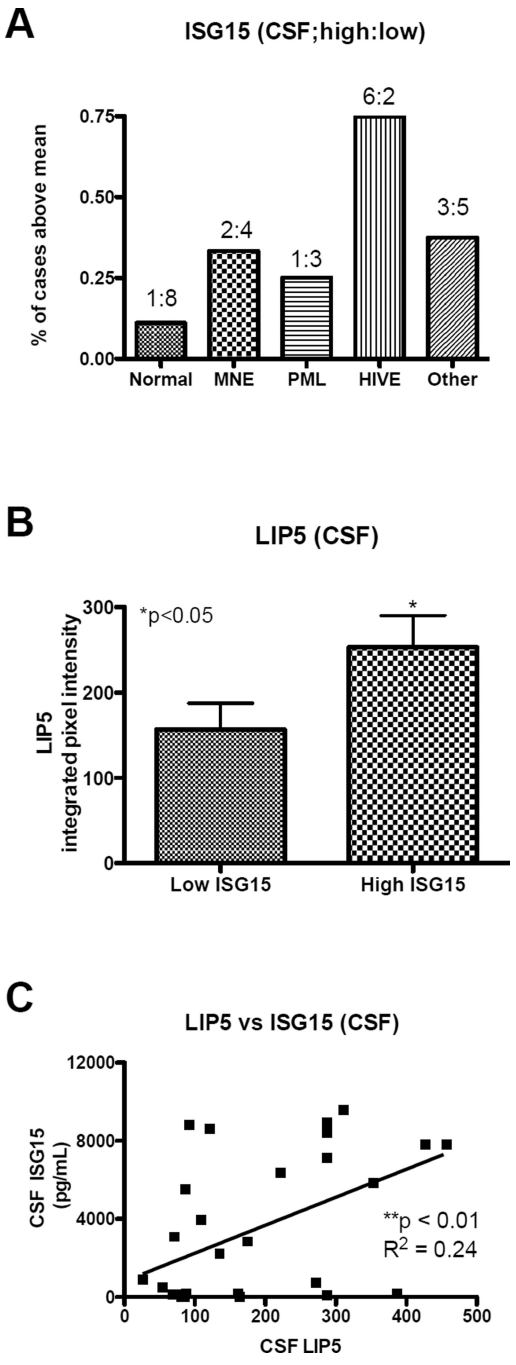

Fig. 2. Elevated CSF ISG-15 in HIVE and concomitant increased CSF LIP-5 expression

A. Graphical representation of the percentage of donors from each neuropathological group to have ISG-15 levels greater than the mean of all cases. **B.** LIP-5 levels in donors with below the mean ISG-15 levels compared to donors with above the mean ISG-15 levels**. C.** Correlation of CSF LIP-5 verses ISG-15 levels in HIV+ donors. A total of n= 35 postmortem cases were analyzed by neuropathological assessment, n= 9 normal, n=6 MNE, n= 4 PML, n= 8 HIVE, n= 8 other. Statistical significance (*p<0.05, One-way ANOVA, post hoc Fisher test, student “T” test or linear regression analysis).

NIH-PA Author Manuscript

NIH-PA Author Manuscript

NIH-PA Author Manuscript

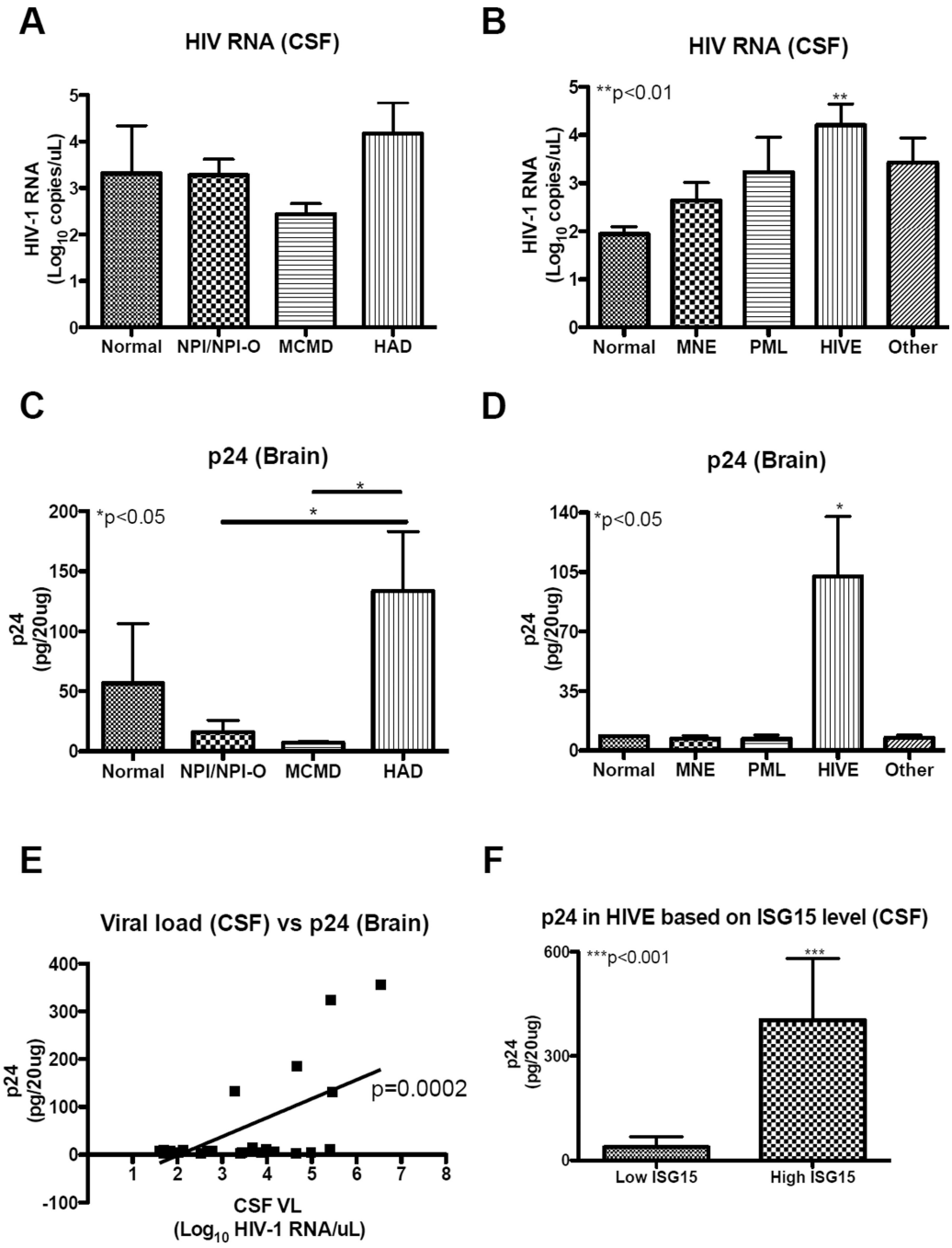

Fig. 3. Increased CNS viral burden coincides with more severe HAND and increased ISG-15 levels

A. CSF HIV-1 RNA expression levels grouped by neurocognitive assessment. **B.** CSF HIV-1 RNA levels grouped by neuropathological diagnosis. **C.** Brain p24 capsid protein levels grouped by neurocognitive assessment. **D.** Brain p24 capsid protein levels grouped by neuropathological diagnosis. **E.** Correlation of CSF HIV-1 RNA quantity versus brain p24 capsid protein levels. **F.** Brain p24 capsid protein levels in donors expressing low or high ISG-15 levels. For statistics, a total of n= 24 postmortem cases were analyzed by neurocognitive impairment, of them n= 3 normal, n= 9 NPI/NPI-O, n= 9 MCMD, n= 3 HAD. A total of n= 35 postmortem cases were analyzed by neuropathological assessment,

n= 9 normal, n=6 MNE, n= 4 PML, n= 8 HIVE, n= 8 other. Statistical significance (*$p<0.05$, One-way ANOVA, post hoc Fisher test, student “T” test or linear regression analysis).

NIH-PA Author Manuscript
NIH-PA Author Manuscript
NIH-PA Author Manuscript

NIH-PA Author Manuscript
NIH-PA Author Manuscript
NIH-PA Author Manuscript

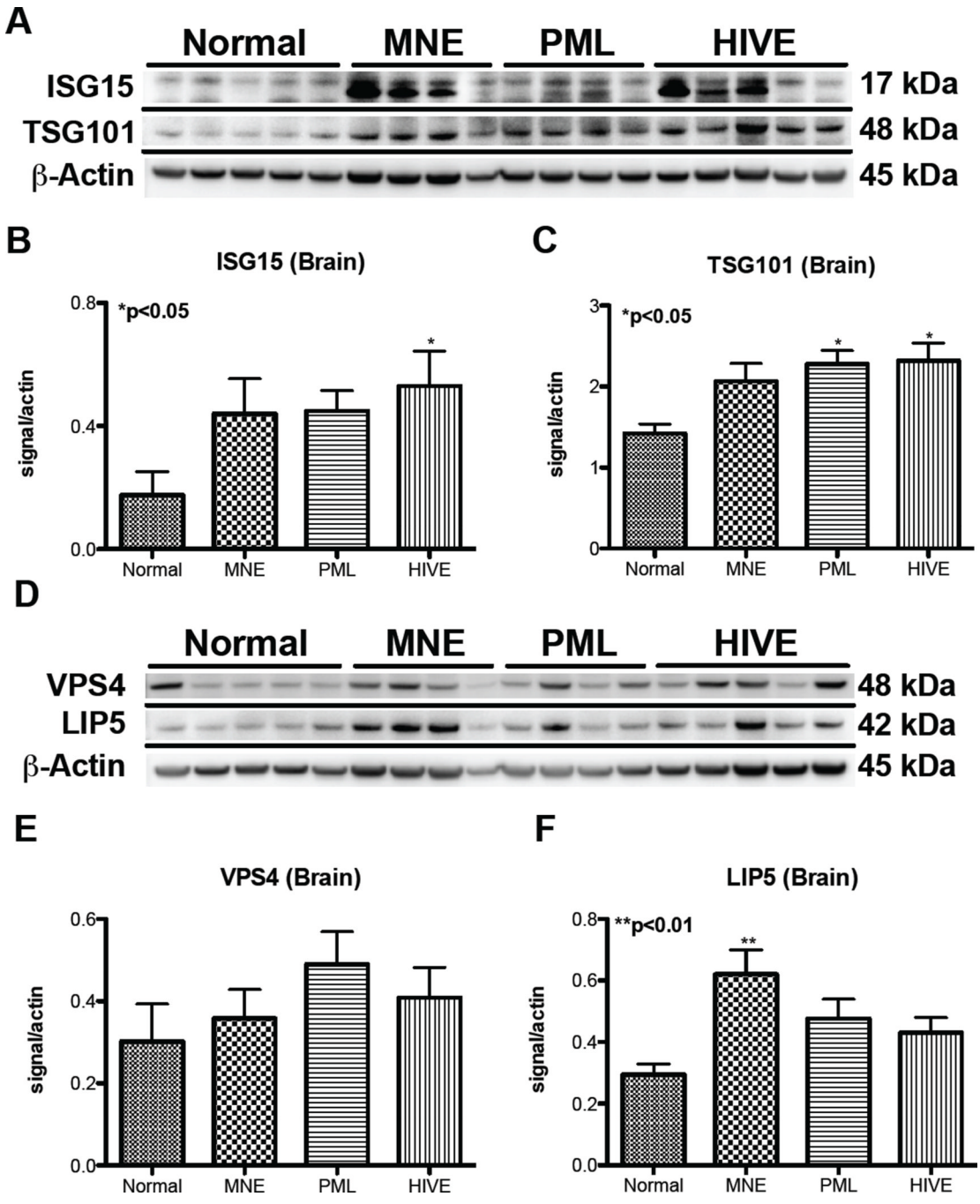

Fig. 4. ESCRT protein levels increase in brain tissues from donors with more severe neuropathological diagnoses

A. Immunoblot analysis of ISG-15, TSG-101 and Actin in postmortem brain tissues from HIV+ donors grouped by neuropathological diagnosis. **B.** Densitometry analysis of ISG-15 levels normalized to Actin. **C.** TSG-101 densitometry analysis normalized to Actin. **D.** Immunoblot analysis of VPS-s and LIP-5 and Actin in postmortem brain tissues from HIV+ donors grouped by neuropathological diagnosis. **E.** Densitometry analysis of VPS-4 levels normalized to Actin. **F.** LIP-5 densitometry analysis normalized to Actin. A total of n= 18 postmortem cases were grouped by neuropathological assessment, n= 5 normal, n= 4 MNE,

n= 4 PML, n= 5 HIVE. Statistical significance (*p<0.05, One-way ANOVA, post hoc Fisher test).

NIH-PA Author Manuscript
NIH-PA Author Manuscript
NIH-PA Author Manuscript

NIH-PA Author Manuscript
NIH-PA Author Manuscript
NIH-PA Author Manuscript

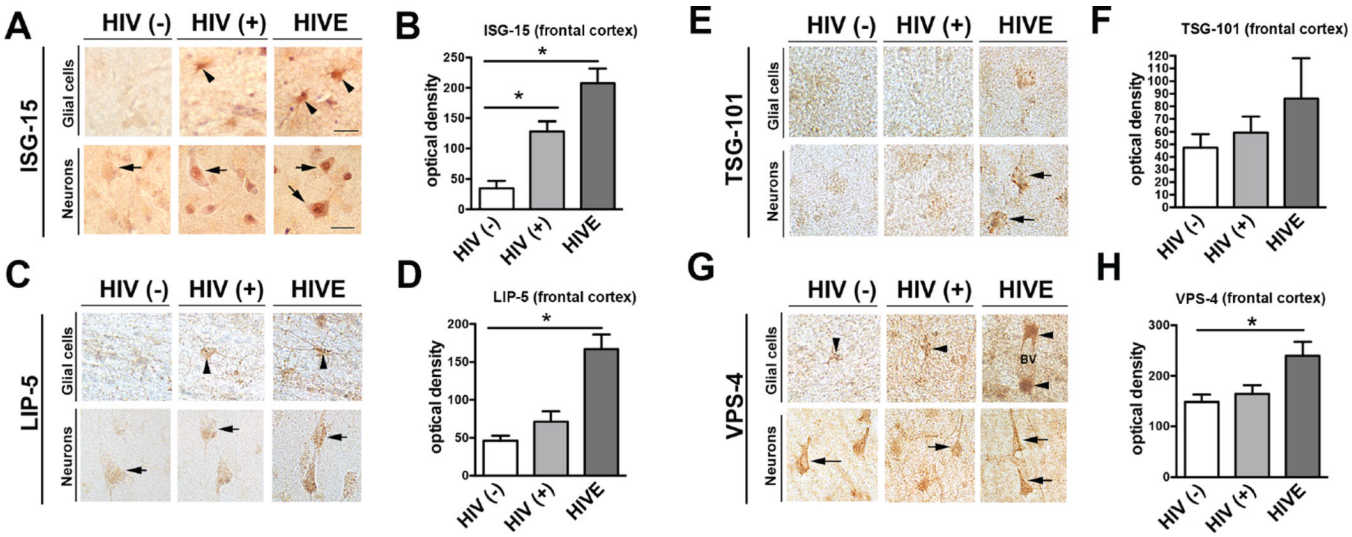

Fig. 5. ESCRT protein immunostaining is increased in brains of HIV+ and HIVE compared to uninfected patients

A. Immunohistochemical analysis of ISG-15 expression in control, HIV+ and HIVE brains. **B.** ISG-15 immunostaining optical density in control, HIV and HIVE brains. **C.** Immunohistochemical analysis of LIP-5 expression in control, HIV+ and HIVE brains. **D.** Optical density of LIP-5 immunostaining in control, HIV and HIVE brains. **E.** Immunohistochemical analysis of TSG-101 expression in control, HIV+ and HIVE brains. **F.** Optical density of TSG-101 immunostaining in control, HIV and HIVE brains. **G.** Immunohistochemical analysis of VPS-4 expression in control, HIV+ and HIVE brains. **H.** VPS-4 immunostaining optical density in control, HIV and HIVE brains. A total of n= 9 postmortem cases were grouped by neuropathological assessment, n= 3 HIV-, n= 3 HIV+, n= 3 HIVE. Statistical significance (*$p<0.05$, One-way ANOVA, post hoc Fisher test).

NIH-PA Author Manuscript
NIH-PA Author Manuscript
NIH-PA Author Manuscript

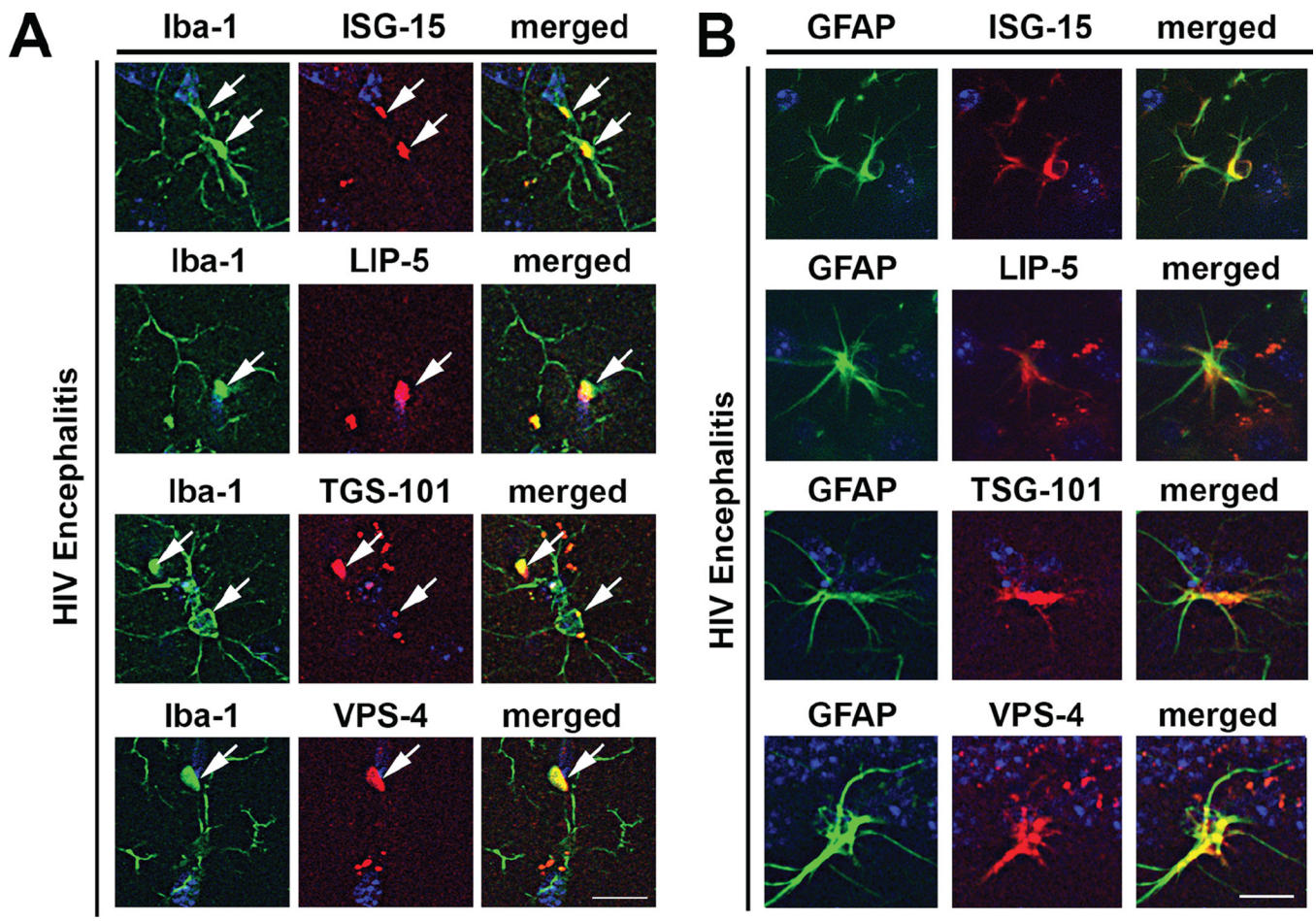

Fig. 6. Double labeling between ESCRT protein and microglia and astrocyte markers in HIVE brains

Vibratome sections from frontal cortex of HIVE patients were double-labeled with antibody against Iba-1 (microglia) or GFAP (astroglia) and ESCRT proteins and analyzed with the laser-scanning confocal microscope. **A.** Colocalization between ESCRT proteins (ISG-15, LIP-5, TSG-101 and VPS-4; red) labeling of Iba-1+ (green) cells in HIVE brain frontal cortex tissue illustrates expression in the microglia cell body. Colocalization is signified by yellow. **B.** Colocalization between ESCRT proteins (ISG-15, LIP-5, TSG-101 and VPS-4; red) and GFAP+ (green) cells in HIVE brain frontal cortex tissue. The yellow signal in the merged channel signifies concomitant red and green staining in GFAP+ cells (astroglia). (Bar = 10 μm)

NIH-PA Author Manuscript

NIH-PA Author Manuscript

NIH-PA Author Manuscript

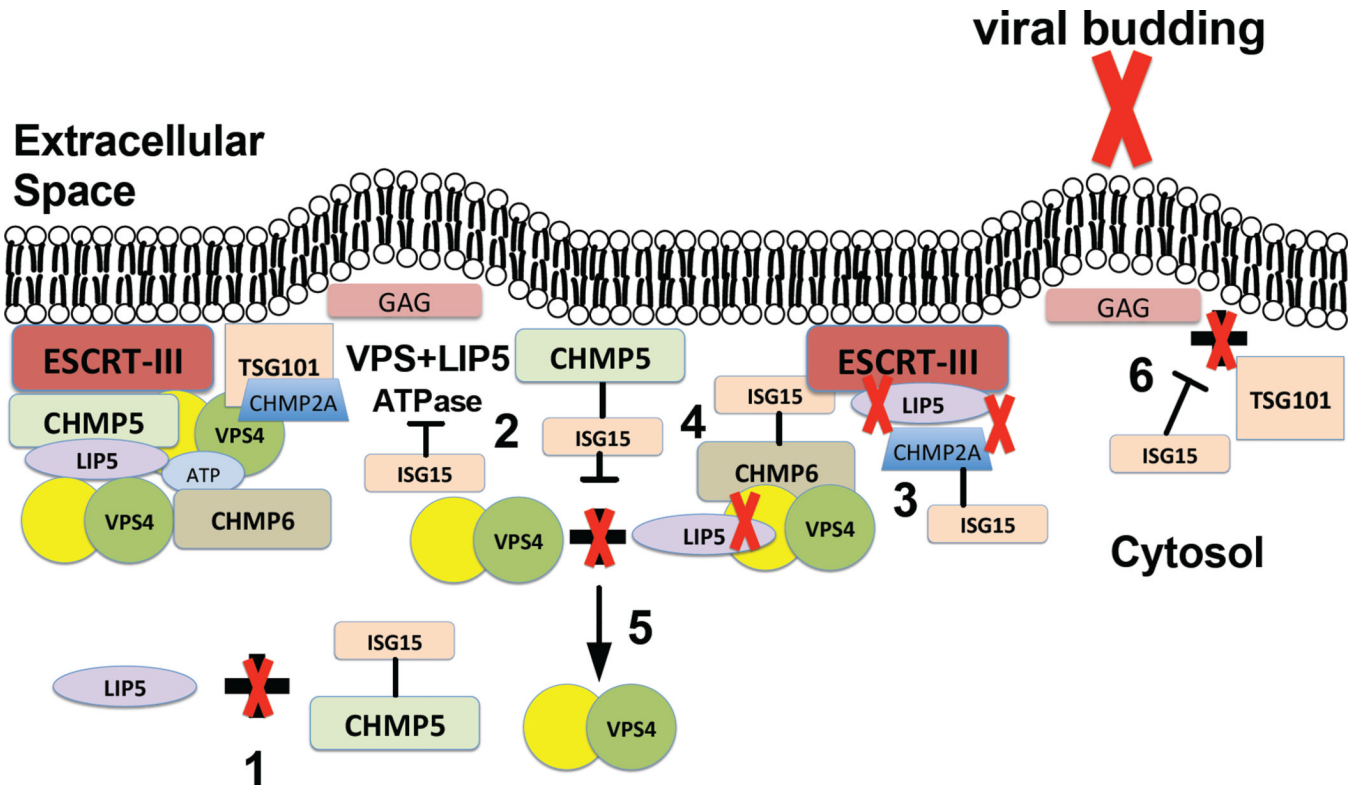

Fig. 7. ESCRT pathway; HIV induces ISG-15 to prevent viral replication

This diagram illustrates the major components of the ESCRT pathway hijacked by HIV-1 to facilitate viral replication. ISG-15 is expressed in response to viral infection, and disrupts proper ESCRT pathway function by binding to, and preventing essential associations necessary for vesicle/virus budding. **1)** ISG-15 is conjugated to CHMP5 thereby preventing LIP-5:CHMP5 association and subsequent localization to the plasma membrane. **2)** Lack of LIP-5:CHMP5 at the plasma membrane prevents VPS-4 associating with its coactivator, LIP-5 and ATPase activity that is essential for virus release. **3)** CHMP2A is ISGylated in the presence of CHMP5:ISG-15, which prevents CHMP2A binding to LIP-5 and VPS-4. **4)** CHMP6 is ISGylated thereby weakening association with VPS-4. **5)** Unbound VPS-4 is released to the cytosol, and viral budding is inhibited. **6)** ISG15 expression prevents TSG101 interaction with GAG, and thereby prevents viral budding.

NIH-PA Author Manuscript
NIH-PA Author Manuscript
NIH-PA Author Manuscript

Table 1

Clinical characteristics of the postmortem samples

Neurocognitive Group	Age (yrs±SD)	N=	Gender M/F	Brain Weight, g	PMT	Log Viral Load (Serum)	Log Viral Load (CSF)	Nadir CD4
Normal	45.3 ± 8.8	8	8/0	1429 ± 165	24.7 ± 42.4	3.75 ± 1.98	3.32 ± 2.29	34 ± 55
NPI/NPI-O	44.8 ± 9.3	19	16/3	1309 ± 130	20.0 ± 21.4	4.13 ± 1.44	3.28 ± 1.46	43 ± 53
MCMD	40.0 ± 6.5	13	12/1	1318 ± 171	13.4 ± 11.0	4.63 ± 1.38	2.44 ± 0.78	30 ± 80
HAD	42.6 ± 7.2	7	6/1	1283 ± 198	9.0 ± 3.5	4.38 ± 1.87	4.17 ± 1.48	30 ± 43

NIH-PA Author Manuscript
NIH-PA Author Manuscript
NIH-PA Author Manuscript

Table 2

Neuropathology of postmortem samples

Neurocognitive Group	N=	Normal	Microglial Nodule Encephalitis	Progressive Multifocal Leukoencephalopathy	HIV Encephalitis	Other	ARV (Y/N)
Normal	8	2 (25%)	0 (0%)	1 (13%)	4 (50%)	1 (13%)	8/0
NPI/NPI-O	19	4 (21%)	1 (5%)	3 (16%)	5 (26%)	6 (32%)	15/4
MCMD	13	4 (31%)	4 (31%)	0 (0%)	1 (8%)	4 (31%)	12/1
HAD	7	0 (0%)	1 (14%)	1 (14%)	4 (57%)	1 (14%)	5/3

NIH-PA Author Manuscript
NIH-PA Author Manuscript
NIH-PA Author Manuscript

Table 3

Independent variables and generated coefficients.

Coefficients						
Model		Unstandardized Coefficients		Standardized Coefficients	t	Significance
		B	Std. Error	Beta		
1	(Constant)	−0.856	0.945		−0.906	0.383
	ISG15	1.774	1.152	0.339	1.54	0.15
	vps4	1.529	1.433	0.219	1.067	0.307
	lip5	−1.456	1.601	−0.204	−0.909	0.381
	tsg101	1.329	0.444	0.611	2.994	0.011

[a]Dependent Variable: Neuropathology

NIH-PA Author Manuscript
NIH-PA Author Manuscript
NIH-PA Author Manuscript

Table 4

ANOVA results and significance.

ANOVA						
Model		**Sum of Squares**	**df**	**Mean Square**	**F**	**Significance**
1	Regression	13.82	4	3.455	4.997	.013[b]
	Residual	8.297	12	0.691		
	Total	22.118	16			

[a] Dependent Variable: Neuropathology

[b] Predictors: (Constant), tsg101, vps4, ISG15, lip5

NIH-PA Author Manuscript

NIH-PA Author Manuscript

NIH-PA Author Manuscript

Table 5

Model summary including R square.

Model Summary				
Model	**R**	**R Square**	**Adjusted R Square**	**Std. Error of the Estimate**
1	.790[a]	0.625	0.5	0.8315

[a]Predictors: (Constant), tsg101, vps4, ISG15, lip5